Atmospheric Environment 279 (2022) 119099

Contents lists available at ScienceDirect

Atmospheric Environment

journal homepage: www.elsevier.com/locate/atmosenv

Investigating sources of surface ozone in central Europe during the hot summer in 2018: High temperatures, but not so high ozone

Hossein Zohdirad [a], Jianhui Jiang [b,c,*], Sebnem Aksoyoglu [c], Masoud Montazeri Namin [a], Khosro Ashrafi [d], André S.H. Prévôt [c]

[a] School of Civil Engineering, College of Engineering, University of Tehran, Tehran, Iran
[b] Shanghai Key Lab for Urban Ecological Processes and Eco-Restoration, School of Ecological and Environmental Sciences, East China Normal University, 200241, Shanghai, China
[c] Laboratory of Atmospheric Chemistry, Paul Scherrer Institute, Villigen, Switzerland
[d] School of Environment, College of Engineering, University of Tehran, Tehran, Iran

HIGHLIGHTS

- Sources of ozone in central Europe in summer 2018 are modeled by CAMx-OSAT.
- Effects of reduced emissions since 2000 and meteorology on ozone are investigated.
- Meteorological conditions in 2018 bring the highest air mass from high ozone areas.
- Reduced anthropogenic emissions are reason for the not-so-high ozone in hot summer.
- The reduced emissions from road traffic contribute most to the decrease of ozone.

ARTICLE INFO

Keywords:
Tropospheric ozone
Source apportionment
CAMx-OSAT
Source contribution
Regional contribution

ABSTRACT

The changing emissions and climate have largely influenced the contribution of different sources on surface ozone, while the relations between the emissions, meteorological conditions and ozone sources are highly uncertain. In this study we modeled the sources of surface ozone in central Europe in the summer (June–July–August) of 2018, one of the warmest summers in Europe, with the regional chemical transport model CAMx and its source apportionment tool OSAT. Additional simulations with the anthropogenic emissions in 2000 were performed as high-emission scenarios to investigate the effects of reduced emissions on ozone sources, and a specific analysis on the coupled effects from meteorology was conducted based on measurements and backward trajectory calculations at three Swiss sites. The model results indicate that the highest contribution to summer afternoon surface ozone in Europe in 2018 comes from the boundary import (65%), followed by off-road traffic (11%) and road traffic (8%). Compared to the case using 2000 emissions, the lower emissions in 2018 lead to lower ozone in most of the areas in Europe except for some urban areas and shipping routes, and the highest decrease is from the road traffic for both the whole domain and the Swiss sites. The backward trajectory analysis at Swiss sites in 2000 (base year), 2003 (the warmest year) and 2018 (the 3rd warmest year) show that 2018 is the year with the highest fraction of air mass from the high ozone areas (from east in southern Switzerland and from north in northern Switzerland). The results indicate that the reduced anthropogenic emissions are the main reason responsible for the reduced high level ozone in the hot summer in central Europe.

1. Introduction

Tropospheric ozone is a strong oxidant and has adverse effects on human health (Li et al., 2012; WHO, 2013) and vegetation (Teixeira et al., 2011). Surface ozone is a secondary pollutant formed by its precursors' chemical reactions in the presence of sunlight in a complicated,

* Corresponding author. Shanghai Key Lab for Urban Ecological Processes and Eco-Restoration, School of Ecological and Environmental Sciences, East China Normal University, 200241, Shanghai, China.
E-mail address: jhjiang@des.ecnu.edu.cn (J. Jiang).

https://doi.org/10.1016/j.atmosenv.2022.119099
Received 5 September 2021; Received in revised form 18 February 2022; Accepted 2 April 2022
Available online 19 April 2022

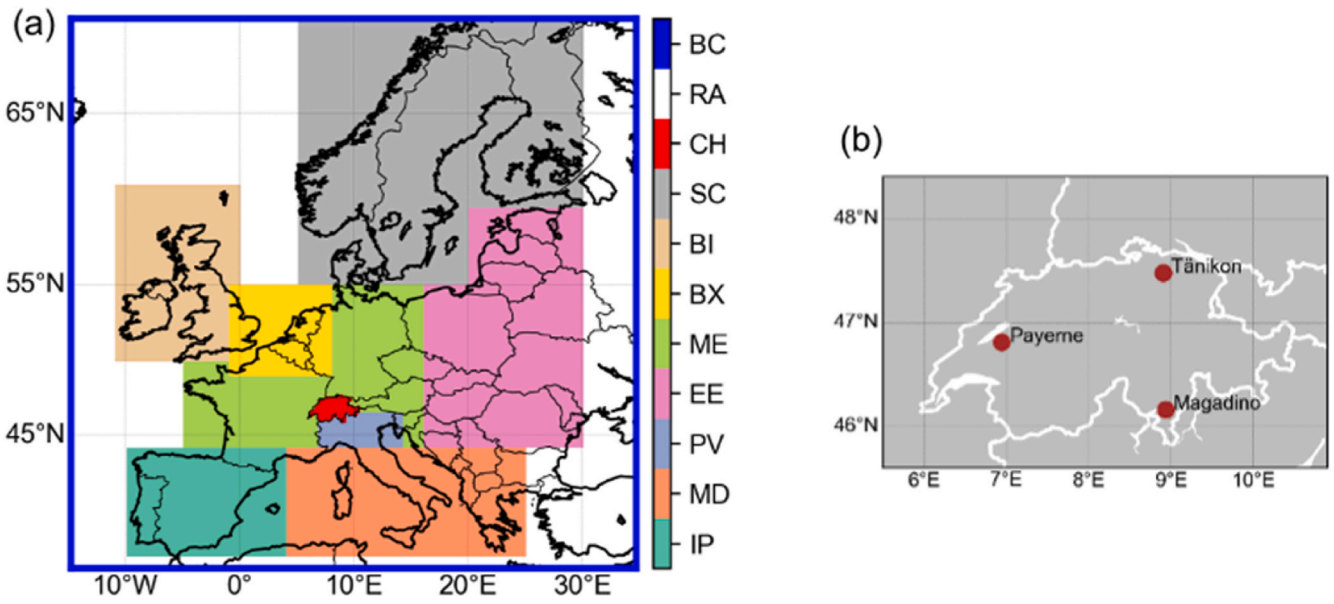

Fig. 1. The model domain and its sub-regions (a) and location of the three receptor sites in Switzerland (b). IP: the Iberian Peninsula, MD: the Mediterranean, PV: Po Valley, EE: eastern Europe, ME: mid-Europe, BX: Benelux, BI: Great Britain & Ireland, SC: Scandinavia, CH: Switzerland, RA: Rest of the area, BC: boundary conditions.

non-linear way (Monks, 2005). The main ozone precursors contributing to the ozone formation are nitrogen oxides (NO_x = NO + NO_2) and volatile organic compounds (VOCs), which have anthropogenic (industries, road vehicles, ships, etc.) and natural emission sources (plants, soil, etc.) (Oikonomakis et al., 2018). Surface ozone concentration can be influenced by controlling the emission of its precursors. Emission control measures applied to ozone precursors non-methane volatile organic compounds (NMVOC) and NO_x during the last three decades in Europe resulted in declining peak ozone levels in rural areas (Colette et al., 2011; Derwent et al., 2010; Guerreiro et al., 2014; Henschel et al., 2015; Jenkin, 2008; Jonson et al., 2006; Monks et al., 2015). Although peak ozone levels decreased, ozone concentrations still often exceed the hourly standard of 120 μg m^{-3} during hot summer periods (Aksoyoglu et al., 2014; Boleti et al., 2018). There is also a strong dependency of surface ozone concentration on meteorology. Temperature and solar radiation are two meteorological parameters that can directly affect the ozone chemistry. High temperature and strong solar radiation lead to high ozone concentrations especially during low-wind periods (Jacob and Winner, 2009; Ordóñez et al., 2005). It therefore becomes important to understand how the meteorological conditions influence the effects of reduced emissions on the sources of surface ozone, especially in the context of increasing occurrence of extreme weather.

Various approaches have been developed to characterize and quantify the relationship between emission sources and ozone concentrations, including the statistical methods, model sensitivity simulations (also known as perturbation method) and model source apportionment approaches (also known as tagging method) (Cohan and Napelenok, 2011; Kwok et al., 2015; Mertens et al., 2020). Of these methods, only model source apportionment methods can completely determine the share of each contributor (emission sectors, geographical regions or other measures) to ozone budget in a practical and inexpensive way (Karamchandani et al., 2017; Kwok et al., 2015; Mertens et al., 2018, 2020). Nevertheless, only few studies investigated the relationships between ozone and its precursors' emissions in Europe using model source apportionment. Tagging approach has been applied in different global (Derwent et al., 2015; Hess and Zbinden, 2013; Mertens et al., 2020; Sudo and Akimoto, 2007) and regional (Borrego et al., 2016; Brandt et al., 2013; Jonson et al., 2018; Karamchandani et al., 2017; Lupaşcu and Butler, 2019; Pay et al., 2018, 2019; Safieddine et al., 2014; Valverde et al., 2016) chemical transport models by previous studies to investigate surface ozone across Europe. Studies investigated the contribution of different source types across Europe generally reported that the main contributors to the high ozone episodes during summer are biogenic emissions and combined transportation section (generally higher on-road contribution than those from off-road transport sector) after non-European emissions (Borrego et al., 2016; Karamchandani et al., 2017; Mertens et al., 2020; Pay et al., 2019; Valverde et al., 2016) but energy and industry sector (Coelho et al., 2017; Karamchandani et al., 2017; Pay et al., 2019), residential sector (Borrego et al., 2016) and solvents (Coelho et al., 2017) were also identified as major contributors by some studies. Investigations in different regions of Europe reported that the summer O_3 is dominated by national and intra-European sources and contribution of non-European emissions are larger for annually averaged ozone (Derwent et al., 2015; Jonson et al., 2018; Lupaşcu and Butler, 2019; Sudo and Akimoto, 2007). More localized studies inside Europe generally blame transboundary transport and regional sources for their high levels of ozone in summertime (Borrego et al., 2016; Coelho et al., 2017; de Cámara et al., 2018; Valverde et al., 2016). However, none of the previous studies applied model source apportionment together with meteorology analysis to describe the ozone status and its variation in Europe.

In central Europe, the year of 2018 was the third warmest summer during the last 150 years according to the measurements (after the summers 2003 and 2015) (CH2018, 2018; Schär et al., 2004). The situation in 2018, however, was rather unusual. Although measured ozone concentrations were above the concentration limits (120 μg m^{-3}) at some sites, the number of days exceeding the "population information threshold" level of 180 μg m^{-3} were fewer than those in the previous hot years. The aim of this study is to understand the ozone situation in 2018 by investigating the ozone sources and effects of meteorological conditions on ozone formation. The source apportionment of surface ozone was conducted by the Ozone Source Apportionment Technology (OSAT) tool of the air quality model CAMx, and the effects of meteorological conditions were analyzed based on measurements and backward trajectory analysis. The paper is organized as follows. In Sect. 2, the data, modeling and analysis methods are introduced; results are given in Sect. 3 beginning with model evaluation and then continuing with comparison of measured surface ozone, temperature and calculated wind regimes in summers 2000, 2003 and 2018, ozone source apportionment investigating the contribution of different source types and regions and

Table 1
Description of the model parameters.

Parameter and inputs	Description
Horizontal resolution	$0.125^{o} \times 0.25^{o}$, latitude-longitude
Vertical resolution	14 layers with variable heights (see the height of each layer in Table S1)
Gas-phase mechanism	Carbon Bond 6 Revision 2 (CB6r2)
Aerosol scheme	SOAP2.1 for organic aerosol chemistry/partitioning; ISORROPIA thermodynamic model for the inorganic aerosols
Deposition scheme	Zhang deposition model
Ozone column densities	TOMS (Total Ozone Mapping Spectrometer) data
Photolysis rates	TUV (Tropospheric Ultraviolet and Visible) Radiation Model
Meteorology	WRF 3.7.1
Initial and boundary conditions	Global model CAM-Chem
Anthropogenic emissions	TNO-MACC-III
Biogenic emissions	PSI-model

Table 2
Description of the simulations.

Simulation name	Year (summer)	Meteorology	Biogenic emissions
s2018	2018	2018	2018
s2018-2NO_x	2018	2018	2018
s2000	2000	2018	2018
s2000-2NO_x	2000	2018	2018

eventually the effects of changes in anthropogenic emissions on ozone since 2000. Conclusions are summarized in Sect. 4.

2. Method

To investigate the effects of reduced emissions and meteorology on surface ozone, we first compared the ozone source apportionment by CAMx-OSAT for different emission scenarios, and analyzed the relation between the ozone concentration and emissions, as well as temperature. The model performance was then evaluated by comparing with the measurements of meteorology and concentrations of air pollutants. Furthermore, a backward trajectory analysis was conducted to investigate the sources of ozone in typical years with distinct meteorological conditions.

2.1. Model setup

The regional chemical transport model CAMx (Comprehensive Air Quality Model with extensions) version 6.5 (Ramboll, 2018) was used to model the air quality. CAMx is a state-of-the-science photochemical transport model used worldwide to simulate the chemical reactions and physical transport (within the domain and across the lateral/upper boundaries) of air pollutants. The model domain covers Europe and it is divided into 11 sub-regions to investigate the contributions of different regions to surface ozone in central Europe (Fig. 1). There are 14 terrain following vertical layers ranging from ~20 m above ground level (first layer) going up to ~8920 m (height of each layer can be found in Table S1). The model parameterization and information about the input data are given in Table 1. The meteorological parameters were prepared by the Weather Research and Forecasting model (WRF) version 3.7.1 (NCAR, 2016), and further processed by WRFCAMx (version 4.411) to provide the inputs required for the CAMx domain. The raw data of initial and boundary conditions were obtained from the global model CAM-Chem (Community Atmosphere Model with Chemistry) by Atmospheric Chemistry Observations and Modeling Laboratory of National Center for Atmospheric Research (UCAR/NCAR). It is at a horizontal resolution of $0.9^{\circ} \times 1.25^{\circ}$ with 56 vertical levels, and the data is saved as instantaneous fields every 6 h. More details about model setup of CAM-Chem can be found in Buchholz et al. (2019). CAM-Chem has been evaluated by NCAR and found to have a positive bias in summertime ozone over Europe, and the bias of the modeled summertime daily 8-h maximum ozone against the observations from EMEP network reached 10–45 ppbv (Lamarque et al., 2012). The raw data was adjusted to the CAMx format by the MOZART2CAMx (version 3.2.1) pre-processor. We adopted the default option of CAMx, the first-order eddy viscosity (K-theory) approach, to simulate the vertical mixing of air pollutants. The vertical diffusivity (*Kv*) fields were derived from the output of the meteorological model WRF based on the YSU method developed by Hong et al. (2006) from Yonsei University. The influence of different vertical mixing schemes and parameters on modeled ozone are reported to be modest, with a difference less than 4% for the modeled 8-h averaged ozone (Tang et al., 2011).

Anthropogenic emissions were based on emission data of 2015 from the high-resolution European emission inventory Monitoring Atmospheric Composition and Climate (MACC)-III by the Netherlands Organization for Applied Scientific Research (TNO), which is an update to TNO-MACC-II (Kuenen et al., 2014). The hourly emissions of NMVOC, SO_2, NO_x, CO, NH_3, PM_{10} and $PM_{2.5}$ from 9 Selected Nomenclature for Air Pollution (SNAP) sources (see Table S2) were generated using annual emissions and temporal variation profiles provided by TNO. The TNO PM-splitting profile was used to split particulate matter emissions. The NMVOC speciation was performed using the approach of Passant (2002) to generate emissions of 20 NMVOC species. Emissions from point sources were distributed to 6 vertical layers using the vertical profile of Bieser et al. (2011). The biogenic emissions (isoprene, monoterpenes, sesquiterpenes and soil NO) were generated by the PSI-model developed at the Laboratory of Atmospheric Chemistry at the Paul Scherrer Institute (Andreani-Aksoyoglu and Keller, 1995; Oderbolz et al., 2013; Jiang et al., 2019). The modeled BVOC emissions by PSI-model were validated in our previous work (Jiang et al., 2019). As an important precursor of ozone, the modeled isoprene concentration by using PSI-model results

Table 3
Statistical results of the model performance evaluation for the daily mean concentrations of the chemical species in summer (June–July–August, JJA) 2018 in Europe and in Switzerland with doubled NO_x (s2018-2NO_x) case. O_3(Aft) represents the mean concentration of ozone in the afternoon (12:00–18:00 UTC). MB: mean bias; ME: mean error; RMSE: root-mean-square error; IOA: index of agreement; MFB: mean fractional; bias; MFE:mean fractional error; r: Pearson correlation coefficient.The units for MB, ME, and RMSE are ppb except for $PM_{2.5}$, which is μg m^{-3}.

Region	Species	No. of stations	MB	ME	RMSE	IOA	MFB(%)	MFE(%)	r (-)
Europe	O_3	309	5	8	11	0.72	13	22	0.57
	$O_{3\ (Aft.)}$	309	3	9	11	0.77	8	19	0.63
	NO_2	347	2	3	4	0.70	29	58	0.57
	$PM_{2.5}$	96	1	4	5	0.74	11	45	0.56
	SO_2	202	−0.1	0.9	1.6	0.37	4	86	0.14
Switzerland	O_3	12	4.5	8.3	10.2	0.67	12	21	0.51
	$O_{3\ (Aft.)}$	12	−2.4	8.1	10.7	0.77	−2	15	0.69
	NO_2	12	−2.6	5.0	6.9	0.45	−28	58	0.12
	$PM_{2.5}$	12	1.3	3.6	4.4	0.62	10	39	0.41
	SO_2	12	0.2	0.2	0.3	0.42	55	72	0.26

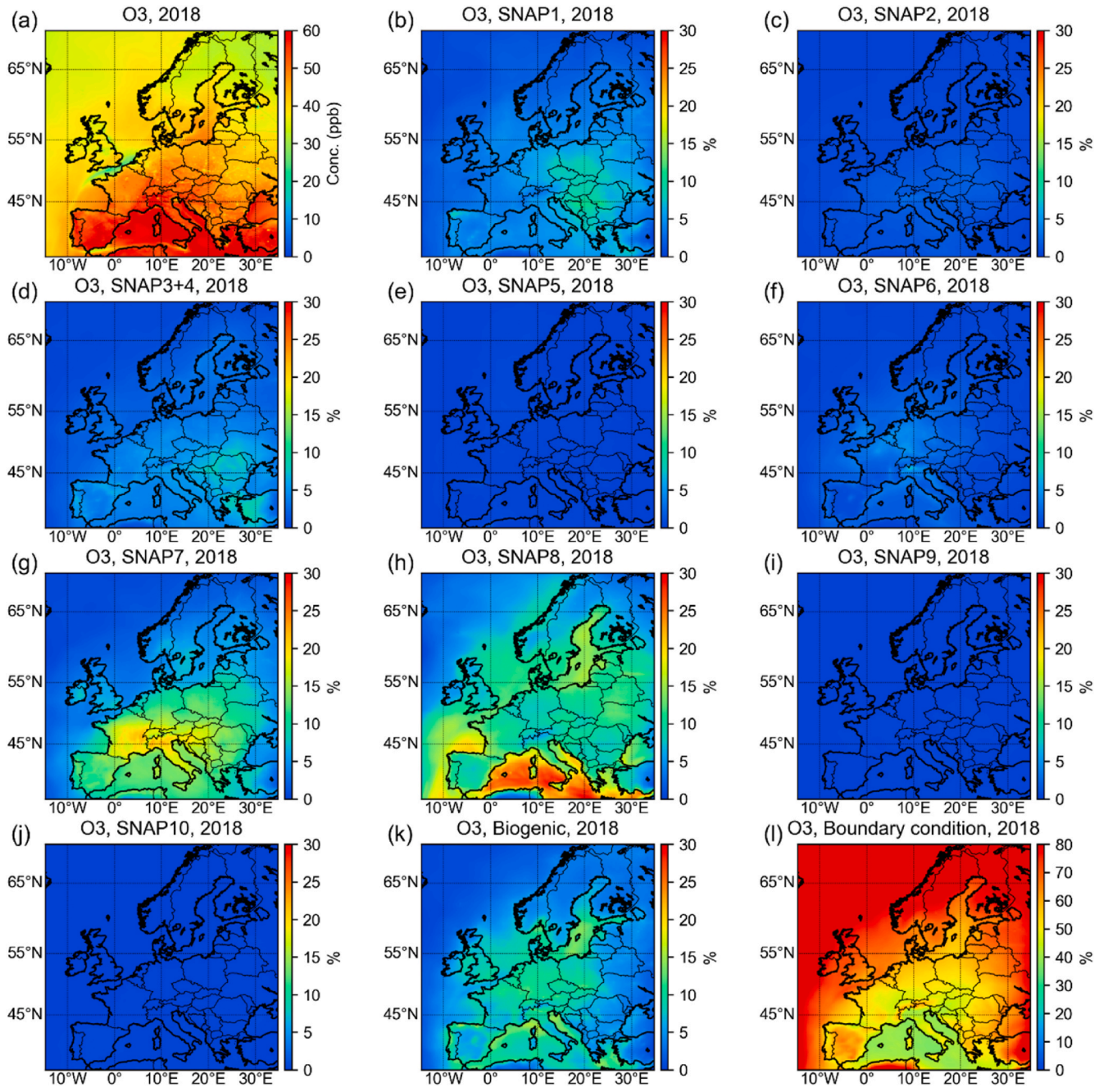

Fig. 2. Modeled daily average ozone mixing ratio (a) and relative contribution of different sources to afternoon ozone mixing ratios across Europe in summer 2018 (s2018-2NO_x) (b-l).

was closer to the measurements in Europe compared to the widely used biogenic model MEGAN v2.1. The other natural emissions such as wildfire and lightning are not included in this study.

The surface ozone concentrations are controlled by both chemical processes and meteorological conditions, and could be influenced by various factors such as emissions, advection, diffusion and entrainment. This study focuses on the influences from the controllable sources, i.e. the anthropogenic emissions. To understand the effects of reduced emissions on surface ozone, we performed another simulation as a reference case with the anthropogenic emissions of 2000 (s2000), which are at a much higher level than in 2018. Meanwhile, our previous study found that the underestimated ozone in Europe potentially come from the underestimated NO_x emissions in Europe, and using the doubled NO_x emissions lead to a better model performance on ozone (Oikonomakis et al., 2018). Therefore, another two simulations with the doubled NO_x emissions (s2018-2NO_x, s2000-2NO_x) were carried as shown in Table 2.

2.2. *Ozone source apportionment: OSAT*

The source apportionment of ozone was carried out using the Ozone Source Apportionment Technology (OSAT) tool of the CAMx model (Ramboll, 2018). It quantifies the source type and source region contributing to ozone at the receptor locations by tracking emission contributions. Additionally, it provides information about whether ozone is formed under NO_x– or VOC– sensitive conditions. The latest OSAT version was improved i) by keeping track of the sources of O_3 removed by reaction with NO to form NO_2 and subsequently returned as O_3 when the NO_2 is photolyzed and ii) by keeping track of NO_x recycling

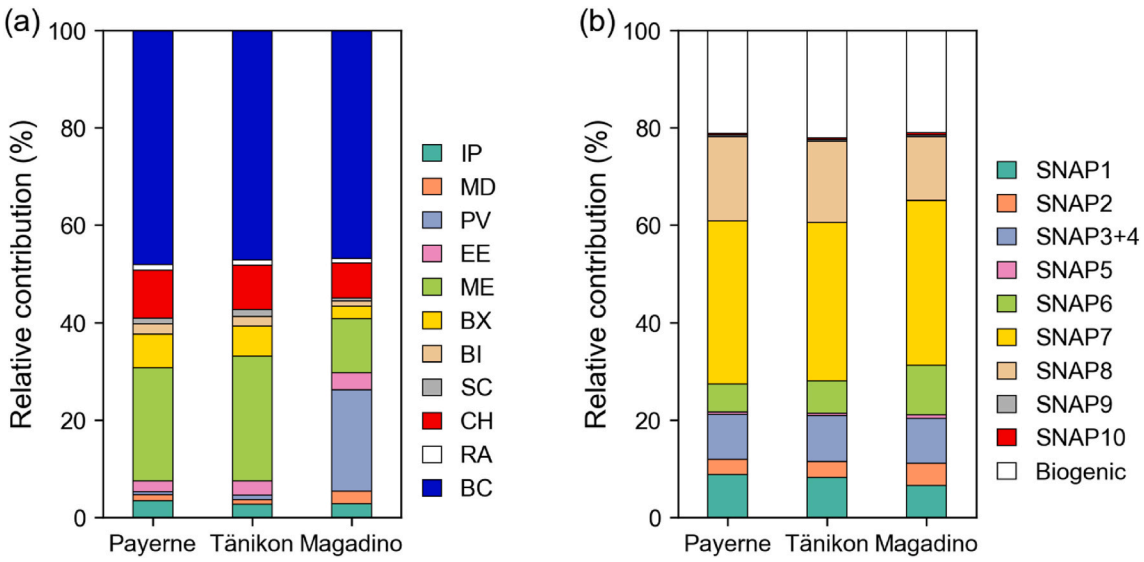

Fig. 3. Relative contribution of different regions (a) and sources (b) to afternoon ozone mixing ratios at Payerne, Tänikon and Magadino in summer 2018 (s2018-2NO_x). IP: the Iberian Peninsula, MD: the Mediterranean, PV: Po Valley, EE: eastern Europe, ME: mid-Europe, BX: Benelux, BI: Great Britain & Ireland, SC: Scandinavia, CH: Switzerland, RA: Rest of the area, BC: boundary conditions.

(Ramboll, 2018). In this study, three rural sites in different regions of Switzerland were selected as receptors of OSAT: Payerne (west), Tänikon (east) and Magadino (south) (Fig. 1b). Contributions from 11 sub-regions (Fig. 1a) and 10 source types (Table S2) including energy industries (SNAP1), non-industrial combustion (SNAP2), industry (SNAP3+4), extraction and distribution of fossil fuels (SNAP5), solvent use (SNAP6), road transport (SNAP7), off-road transport and other mobile sources (SNAP8), waste treatment (SNAP9), agriculture (SNAP10) and biogenic sources (Bio) were traced.

2.3. Model evaluation

The meteorological parameters (surface temperature, wind direction, wind speed, and humidity) modeled by WRF in the whole domain were evaluated using observations obtained from the UK Met Office Integrated Data Archive System (MIDAS) Land Surface Stations database. It covers the measured meteorological data from more than 800 stations in Europe, with a time resolution of 3 h. The model performance of CAMx in predicting the major air pollutants in Europe was evaluated using measurements reported in the Air Quality e-Reporting (AQ e-Reporting) database of the European Environment Agency (https://www.eea.europa.eu/data-and-maps/data/aqereporting-8). A more specific evaluation was conducted for Switzerland by comparing the model results with the measured air quality data at 12 stations (altitude <700 m) from the Swiss National Air Pollution Monitoring Network (NABEL) (Table S3). The air quality and meteorological data for the NABEL stations were obtained from Swiss Federal Office of Environment (BAFU).

2.4. Measurements and backward trajectory analysis

The year 2003 was one of the warmest summers of the last 150 years in central Europe. Therefore, 2003 along with the emission inventory of 2000 were selected for the sake of investigation on the effects of meteorology on the unusual situation of 2018. The measured air quality and meteorological data used for the analysis of differences between summers in different years at three Swiss sites obtained from NABEL stations.

In order to understand the effects of different meteorological conditions, we performed a backward trajectory calculation together with a clustering method (Guo et al., 2009) at the three receptors in the summer of 2000, 2003 and 2018. Lagrangian trajectory calculation module of the NOAA-HYSPLIT model (The Hybrid Single-Particle Lagrangian Integrated Trajectory model) is used to calculate air mass back trajectories. The model considers the time integrated advection of air parcel as a simple trajectory which only requires the three-dimensional velocity field (Draxier and Hess, 1998). The reanalysis data from National Center for Environmental Prediction (NCEP) with 2.5° outputs are used to provide meteorological inputs (ftp://arlftp.arlhq.noaa.gov/pub/archives/reanalysis/), which contains 6-hourly basic meteorological fields on pressure surfaces with the spatial resolution of 2.5°. In this study, the model uses the vertical velocity field in the meteorological data file to calculate trajectory vertical motion and the ending point is set at the level of 2 m above ground level. The 48-h backward trajectories are calculated from July to August for 2000, 2003 and 2018 to find out the pathways of the air masses before reaching Payerne, Tänikon and Magadino. Trajectories that are near each other are merged based on the Euclidean distance clustering method (Wang et al., 2009) and these so-called "clusters" are represented by their mean trajectory.

3. Results and discussion

3.1. Model performance

The statistical parameters from the evaluation of the meteorological inputs (including temperature, wind speed, wind direction, humidity) and the planetary boundary layer height (PBLH) are given in Table S4. The model results generally show a good agreement with the surface observations and meet the performance criteria recommended by Emery et al. (2001). The mean bias of the surface temperature (-0.5 °C) is at the low end of the recommended criteria (<+0.5 °C), mostly due to the underestimation in the Alpine region. The model works well on predicting PBLH with a mean bias ~34 m, which is comparable with other modeling studies in Europe (Oikonomakis et al., 2018; Bessagnet et al., 2016).

The statistical results for the performance of the CAMx on modeling ozone and other major air pollutants in Europe and on Swiss sites are shown in Table 3 for s2018-2NO_x simulation (results for s2018 scenario is shown in Table S5). The model generally performs well on predicting the air quality in Europe, and the statistical results are comparable with other studies for both s2018 and s2018-2NO_x (Bessagnet et al., 2016;

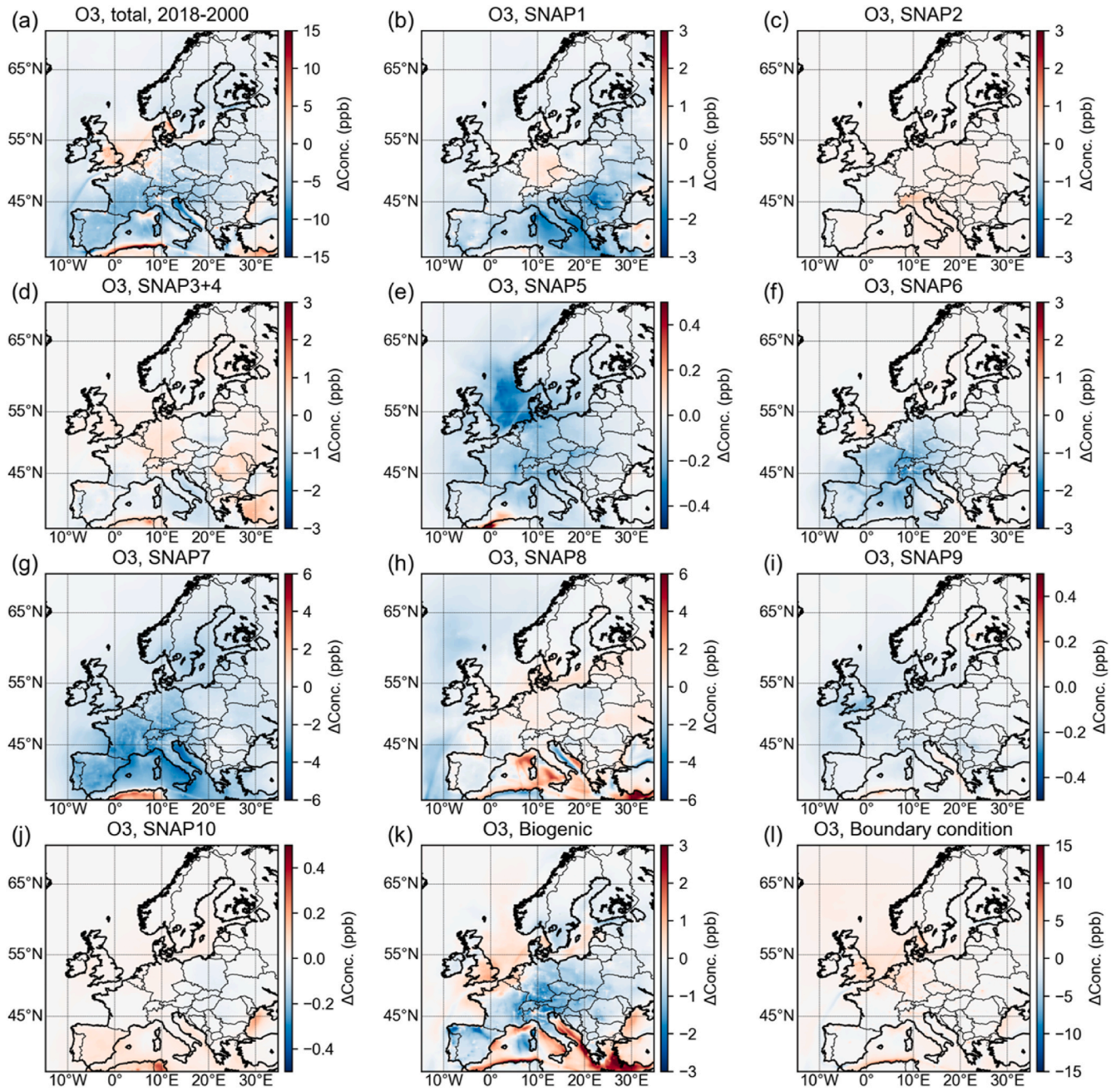

Fig. 4. Change in afternoon average ozone mixing ratio (daily average in Fig. S7) between 2018 and 2000 due to changes in emissions (s2018-2NO_x minus s2000-2NO_x) (a) and contribution of changed emissions from different sources to the change of afternoon ozone mixing ratios.

Jiang et al., 2020; Oikonomakis et al., 2018). The model performance criteria for ozone (MFB $< \pm 30\%$; MFE $< 45\%$) by EPA (2007) and the recommended model performance goal for $PM_{2.5}$ (MFB $< \pm 30\%$; MFE $< 50\%$) by Boylan and Russell (2006) are well met in this study. Although the statistical results are close for s2018 and s2018-2NO_x, the doubled NO_x emission inputs largely improve the situation that the low-level ozone were overestimated and high-level ozone were underestimated (Fig. S1). Comparison of the two cases in Switzerland suggests that model performance for NO_2 and afternoon ozone is improved when NO_x emissions are doubled as suggested by Oikonomakis et al. (2018). The time series of measured and modeled ozone mixing ratios at the three sites in Switzerland also support the improvement with doubled NO_x emissions (see comparison of modeled and measured ozone in Fig. S2). The modeled peak ozone concentrations are closer to the measurements in s2018-2NO_x case.

3.2. Sources of ozone in Europe

As the 2NO_x scenario shows better agreement between the modeled and measured ozone, the analyses in this section are based on the modeled results of the s2018-2NO_x scenario (results for s2018 scenario are shown in Fig. S3). The modeled daily mean ozone concentrations in summer 2018 are shown in Fig. 2a for s2018-2NO_x scenario. The domain average ozone concentration in the summer afternoon reaches 43 ppb, and the highest ozone occurs in the Mediterranean region with a value of 73 ppb. In the southern part of the model domain, ozone levels are higher due to higher temperatures and higher photochemical activity. Lower ozone concentrations, which are clearly visible at polluted regions such as urban areas and shipping routes, are due to titration of ozone with NO.

The source apportionment results over Europe are given in Fig. 2b-l

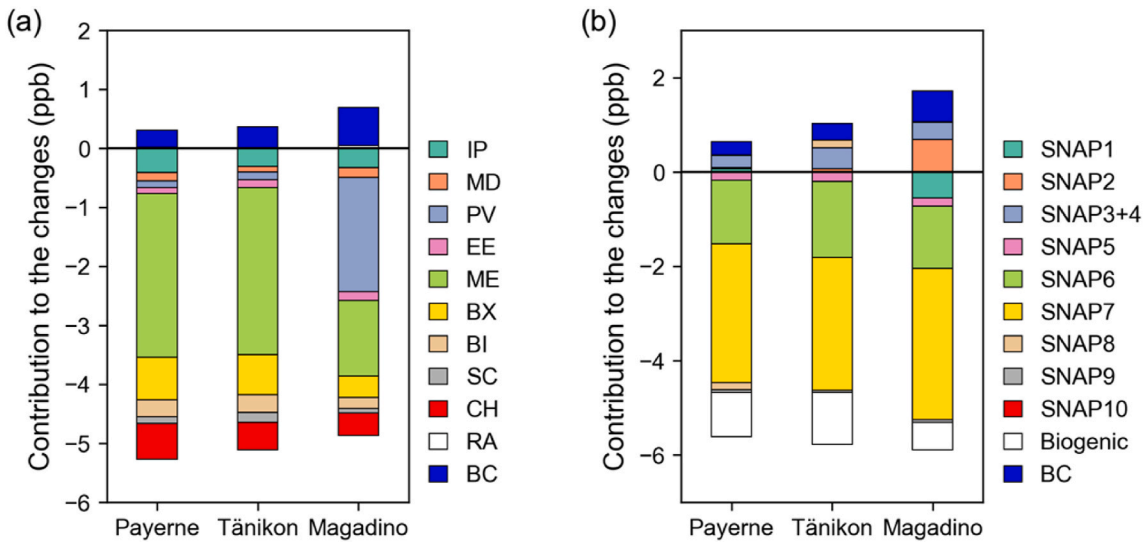

Fig. 5. Contribution of different regions (a) and sources (b) to the change of afternoon ozone mixing ratios at Payerne, Tänikon and Magadino using 2018 and 2000 emissions ($O_{3,2018}$- $O_{3,2000}$). IP: the Iberian Peninsula, MD: the Mediterranean, PV: Po Valley, EE: eastern Europe, ME: mid-Europe, BX: Benelux, BI: Great Britain & Ireland, SC: Scandinavia, CH: Switzerland, RA: Rest of the area, BC: boundary conditions.

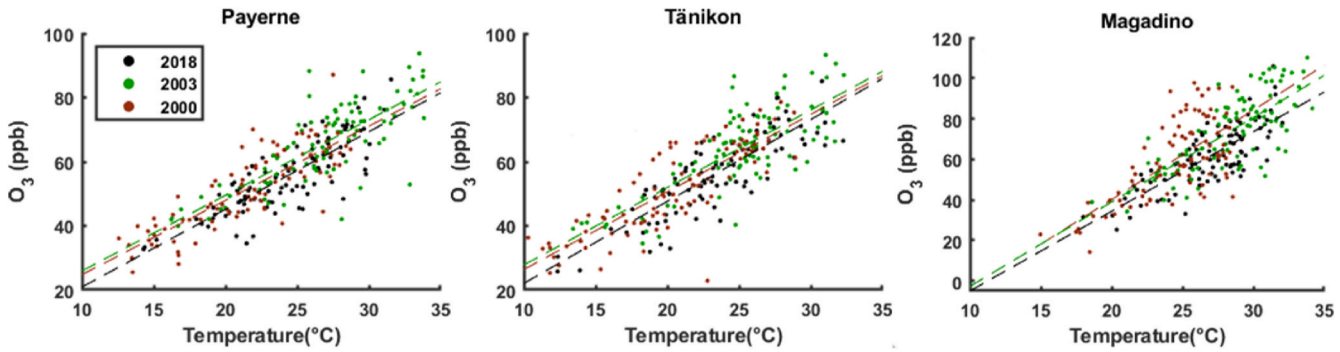

Fig. 6. Relationship between measured surface afternoon (12:00–18:00 UTC) ozone and temperature at Payerne, Tänikon and Magadino in summer 2000, 2003 and 2018. The linear regression lines are shown as dashed lines.

as relative contribution and in Fig. S4 as absolute contribution from different sources. The largest contribution to the surface ozone is import from outside boundary of the domain with an average fraction of 65%, followed by the off-road traffic (11%), road traffic (8%) and the biogenic emissions (6%). The large contribution of the boundary conditions to surface ozone in Europe was also found in previous studies (Pay et al., 2019; Karamchandani et al., 2017; Bessagnet et al., 2016; Andreani-Aksoyoğlu et al., 2008). It is potentially related with the over-predicted summertime ozone of CAM-Chem (Lamarque et al., 2012) – the boundary condition inputs we used, which could also be responsible for the overestimated ozone (Table 3). Besides the boundary conditions, road traffic contributes most to the surface ozone over land, especially in central Europe. As the high NO_x emissions from road traffic in urban area enhance the local NO titration, high ozone levels generally occur in the downwind of the urban area such as the north of Milan. Similar downwind effects were also found during summertime in previous studies (Liu et al., 2007; Pay et al., 2019; Valverde et al., 2016). Ozone generated from the biogenic sources reaches up to ~20% in the coastal area of the Mediterranean Sea, potentially due to the synergistic impact of the interaction between biogenic and anthropogenic sources which could largely increase the peak ozone (Li et al., 2018). The high uncertainties of biogenic emission model could influence the contribution of biogenic sources to surface ozone, but such effects were found to be small as the ozone formation in most regions of Europe is NO_x-sensitive (Jiang et al., 2019). Even in Mediterranean region with high NO_x emissions from shipping, the ~3 times higher isoprene emissions only led to ~10% higher ozone mixing ratio in summer.

A more specific analysis was conducted for Switzerland in central Europe. Fig. 3 shows the relative contribution of regions and sources to summer afternoon ozone concentrations at three Swiss receptor sites in 2018. The main difference between the sites in the north and the south Switzerland is in the regional contribution (Fig. 3a). Apart from the boundary conditions – for which the contribution is similar everywhere at about 47% – central Europe (ME) is the largest contributor to ozone in the north (24%), while the Po Valley contributes more to ozone in the south (21%). The Benelux area contributes more to the sites in the north whereas at Magadino, the contribution from the Mediterranean region is visible. The domestic contribution from Switzerland to ozone at all three sites is similar, but slightly higher in the north (10%) than in the south (7%). Source contributions look quite similar at all three sites (Fig. 3b). The largest contribution (31–34%) comes from road traffic (SNAP7), followed by biogenic emissions (21–23%) and off-road transport (13–18%) with slightly higher contributions from SNAP2 and SNAP6 at Magadino.

3.3. *Effects of changes in anthropogenic emissions*

The effects of changes in anthropogenic emissions on ozone concentrations in Europe are shown in Fig. 4a. The reduced emissions of ozone precursors in 2018 lead to lower ozone in most of the area in

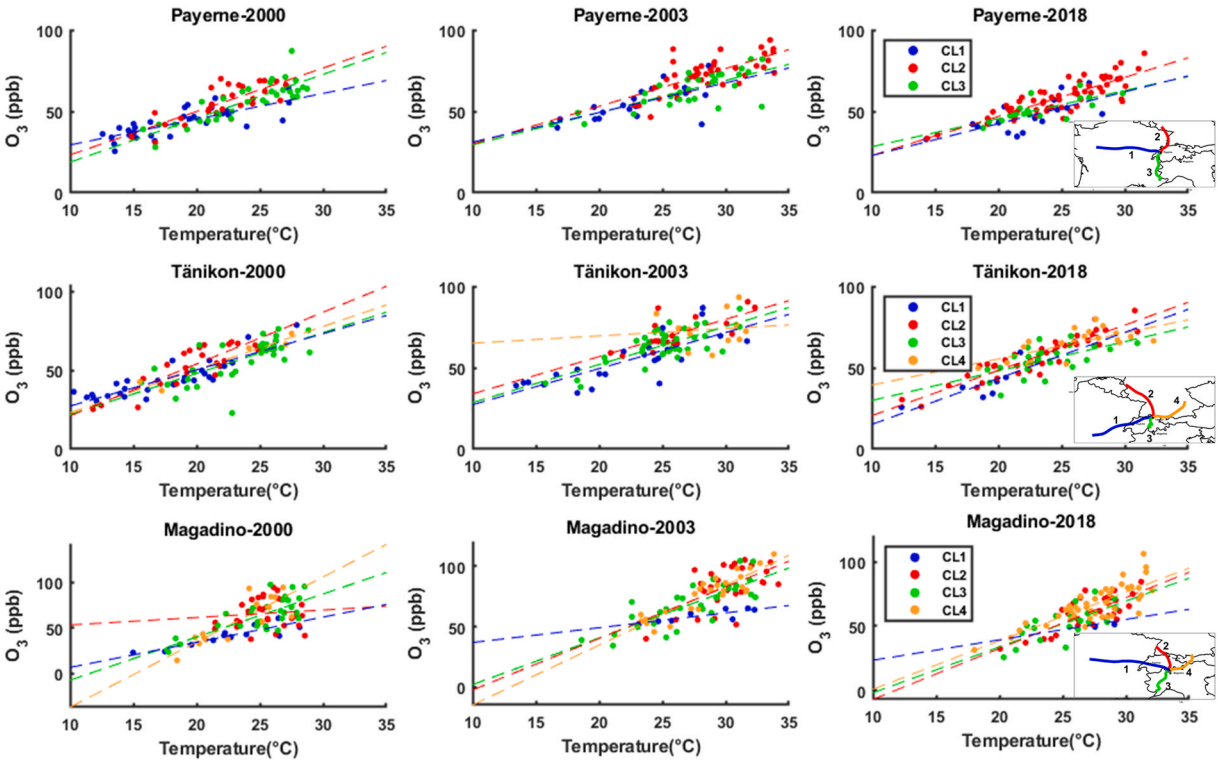

Fig. 7. The relationship between measured surface afternoon (12:00 to 18:00 UTC) ozone and temperature for different trajectory clusters (shown in the insert) at Payerne, Tänikon and Magadino in 2000, 2003 and 2018.

Europe than using the 2000 emissions, while increased ozone occurred around the urban area and along the shipping routes due to the decreased NO titration. A similar situation was also found in our previous study (Jiang et al., 2020). Contribution of different source categories to ozone concentration change from 2000 to 2018 is depicted across Europe in Fig. 4b-l. Road traffic (SNAP7) contributes most to the decrease of ozone using 2018 and 2000 emissions. Ozone from boundary conditions shows the largest increase especially in UK and the Benelux region, potentially derives from the decreased NO titration due to reduced emissions in 2018. Ozone from off-road traffic (SNAP8) increases over the Mediterranean sea in 2018 compared to that using the 2000 emissions, which is largely due to the increase of ship emissions between 2000 and 2018 (Fig. S5). The situation of biogenic ozone is more complicated. Although the biogenic emissions were kept the same in these two cases, ozone from biogenic sources shows a considerable increase over the sea. To further investigate the reason, we compared the modeled biogenic ozone in s2018 and s2018-2NO_x, and found that the increasing NO_x emissions makes the area more VOC-limited for ozone formation, leading to increased effects from biogenic emissions (Fig. S6). This is consistent with the effects of increased NO_x emissions from ships on increasing the biogenic emissions.

Contribution of different regions to ozone concentration change from 2018 to 2000 is depicted for three Swiss receptor sites in Fig. 5a. Mid-Europe (ME) has the largest contribution (~2.80 ppb) to the reduction of surface ozone concentration from 2000 to 2018 in northern Switzerland. This reduction is also significantly affected by Benelux area (~0.70 ppb), domestic contribution (~0.55 ppb) and Iberian Peninsula (~0.35 ppb). In southern Switzerland, the main contributors to the reduction of surface ozone concentrations from 2000 to 2018 are Po valley (~1.90 ppb) and Mid-Europe (~1.30 ppb) beside some regions with lower contributions such as Benelux area (~0.37 ppb) domestic contribution (~0.37 ppb) and Iberian Peninsula (~0.33 ppb). The effects of anthropogenic emissions on ozone at the Swiss sites are displayed in Fig. 5b. Following the highest contribution from road traffic (~2.82 ppb Tänikon to ~2.93 ppb Payerne), contribution of solvent use (SNAP6) to the changes (decrease) of ozone reaches ~1.31 ppb (Magadino) to ~1.61 ppb (Tänikon). There are also high contribution to the change (decrease) of ozone from energy industry (~0.54 ppb) at Magadino. The contribution of industry (SNAP3+4) has an increasing effect on the change of afternoon ozone mixing ratios (~0.36 ppb at Magadino to ~0.44 ppb at Tänikon). This increasing effect is also significant from residential combustion (~0.69 ppb) at Magadino as a result of higher population density in this area.

3.4. *Effects of meteorology*

3.4.1. *Correlation of measured ozone with temperature*

The relationship between the measured afternoon ozone mixing ratios and temperature is shown in Fig. 6. The ozone mixing ratios generally increase with the temperature, but the relation between the ozone and temperature varies with the years and stations. In Magadino which is located in southern Switzerland, the largest slope of the scatter plot occurs in 2000 when the temperature is lowest, whereas the slopes in 2018 are slightly steeper for the northern stations Payerne and Tanikon.

To better understand the reasons for these differences, we analyzed the relationship between ozone and temperature for different trajectory clusters (Fig. 7). The calculated trajectories are clustered in three different groups for Payerne and four different groups for Tänikon and Magadino as shown in Fig. S8 (left panel) together with their contributions throughout the summers of 2000, 2003 and 2018 (right panel). In all of the studied years, the main trajectories were from the west (close to the Atlantic Ocean), north and south in western Switzerland (Payerne) while in the east (Tänikon and Magadino) in addition to the west, north and south trajectories, there was also a trajectory from east which led to the highest ozone concentrations in the southern Switzerland (Po Valley) and significant values in northern Switzerland. At all of the studied sites, the smallest slope (lowest ozone at higher temperatures) is for the trajectory from the west while the north (Belgium, the Netherlands and Germany) and south trajectories led to

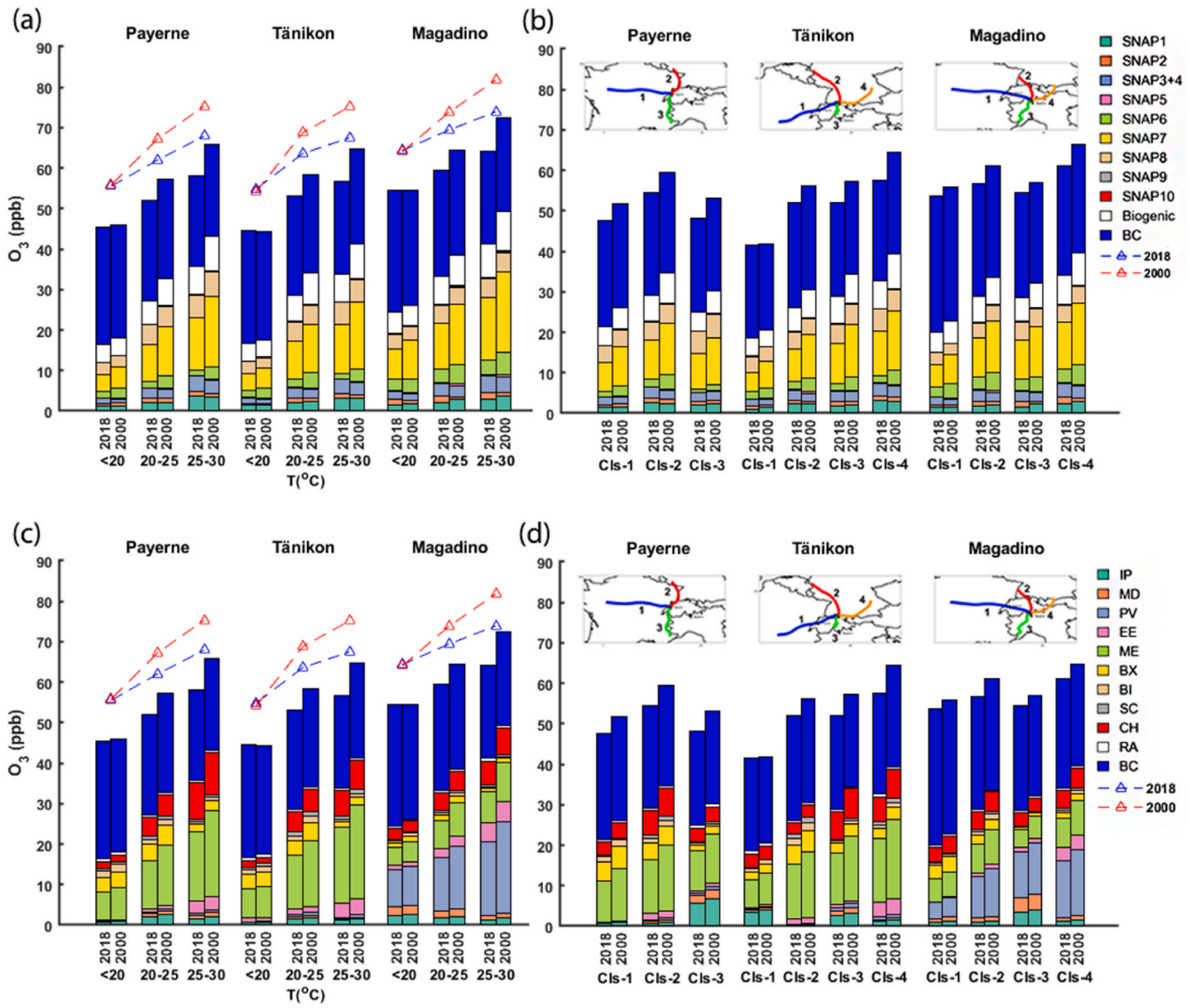

Fig. 8. Variation of the source contributions to the afternoon (12:00–18:00 UTC) ozone mixing ratios with temperature (a) and from different trajectory clusters (b) and variation of the regional contributions to the afternoon (12:00–18:00 UTC) ozone mixing ratios with temperature (c) and from different trajectory clusters (d) at Payerne, Tänikon and Magadino for s2018-2NO_x and s2000-2NO_x scenarios. The lines show the trends of the respective bars and are shifted up by 10 ppb for visualization purposes.

steeper slopes (higher ozone concentrations). From 2000 to 2018, the contribution of trajectory clusters from east in southern Switzerland and from north in northern Switzerland (which led to higher ozone concentration) increased, while the contribution of trajectories from the west bringing clean air masses from the ocean decreased (Fig. S8).

These analyses suggest that the main differences in the meteorological conditions between the summers of 2003 and 2018 were i) higher temperatures in 2003 which leads to higher ozone concentrations relative to 2018, ii) air masses coming from east in southern Switzerland and from north in northern Switzerland, which can lead to higher ozone concentrations, have higher contributions in 2018 relative to 2003.

3.4.2. Variation of source and regional contribution to ozone with temperature and cluster

Increasing temperatures are predicted to increase the source contributions to ozone except from SNAP5, SNAP6 and the boundary conditions (Fig. 8a). In the case of 2NO_x simulations, the changes are larger (see the trend lines above the bars in Fig. 8a and Fig. S8). The contribution of road traffic to ozone increases from 9 to 22% with increasing temperatures in the north while the change is from 13 to 24% in the south.

The increased contributions to ozone at Payerne correspond to the trajectory cluster from north, at Tänikon mainly correspond to the trajectory cluster from east and then north and south, and at Magadino, increased contributions are correlated with both east and north clusters (Fig. 8b). These results are in agreement with those from observations in section 3.2.2. There is no significant change in source contribution of different trajectory clusters at the studied sites.

The contribution to ozone at Payerne and Tänikon from northern regions such as the Benelux area, Great Britain & Ireland decreases with increasing temperature, while the Swiss and central European contributions increase (Fig. 8c). The reason for this is probably the stagnant conditions with very low winds during hot days. At Magadino, on the other hand, the contribution from the Po Valley, Switzerland, central Europe and eastern Europe increases, but the contribution from the Mediterranean region decreases.

The contributions of various regions to the afternoon ozone at Payerne, Tänikon and Magadino for different trajectory clusters are

shown in Fig. 8c. At Payerne, the highest ozone levels are in the north cluster (cluster 2) in which contributions from central Europe (ME), Switzerland (CH), Benelux area and eastern Europe (EE) are larger than those in cluster 3 (south), where the contributions from the Mediterranean (MD) and Iberian Peninsula (IP) can be seen. At Tänikon, where the highest ozone is in the east, south and north clusters, respectively, the common main contributors are central Europe (ME), Switzerland (CH) and Benelux area. However, the Swiss contribution is lower and Benelux contribution is larger at north cluster. There is larger contribution from central Europe (ME) in east cluster and the contributions from the Mediterranean (MD) and Iberian Peninsula (IP) can be seen in south cluster. In the south, at Magadino, the east and north cluster leads to the highest ozone levels, as in the north. In this case, however, the largest contribution comes from Po Valley (PV), followed by central Europe, Switzerland and eastern Europe.

4. Conclusions

The aim of this study is to understand the ozone situation in the summer of 2018 in central Europe using the regional chemical transport model CAMx and its source apportionment tool OSAT. We calculated the contributions from different emission sources to ozone concentrations across Europe, and a specific case study was conducted at three rural receptor sites in Switzerland: Payerne (west), Tänikon (east) and Magadino (south). Additional simulations were performed with the anthropogenic emissions in the year 2000 and the same meteorology as 2018 to investigate the effects of decreased precursor emissions on the changes in ozone. In order to understand the effects of meteorological conditions, we used a backward trajectory calculation together with a clustering method at the three Swiss sites in 2018, as well as 2000 (as a base case) and 2003 (as a reference year with the warmest summer of the last 150 years in central Europe). The model results indicated that the most important sources for ground-level ozone in Europe during summer 2018 are the boundary conditions (65%), followed by the off-road traffic (11%), road traffic (8%) and the biogenic emissions (6%). Besides the boundary conditions, road traffic contributes most to the surface ozone over land in central Europe. In Switzerland, a significant contribution (~47%) to ozone is from the boundary conditions for all the receptors. The contributions from different emission sources to the ozone concentrations are similar at all receptor sites, with road traffic (SNAP7) being the largest contributor (31–34%) besides boundary conditions, followed by biogenic emissions (21–23%) and off-road transport (SNAP8) (13–18%). At Payerne and Tänikon, about 30% of the ozone originated in central Europe and the Benelux area, while their contributions drop to about 15% in the south, at Magadino, where the contribution from the Po Valley is 21%.

The comparison between simulations with 2018 and 2000 emissions shows that reduced emissions of ozone precursors in 2018 lead to lower ozone in most of the area in Europe than using the 2000 emissions, except for the urban areas and along the shipping routes where increased ozone is found due to the decreased NO titration. At the Swiss sites, the reduced emissions from road traffic contribute most (2.82 ppb–2.93 ppb) to the decrease of surface ozone, followed by the reduced emissions from solvent use (1.31 ppb–1.61 ppb). Although the same biogenic emissions were used in the simulations, the ozone from biogenic sources decreased by 0.28 ppb–0.64 ppb when using 2018 emissions, potentially due to the decreased NO_x precursors overall. Largest regional contributions to the change (reduction) of surface ozone by using 2000 and 2018 emissions in northern Switzerland are found to belong to Central Europe, Benelux area, Switzerland and Iberian Peninsula (in south trajectory cluster). In southern Switzerland, the largest contributions to the reduction of surface ozone are Po valley, Central Europe, Switzerland and Iberian Peninsula.

Analyses of the measurements and the backward trajectories in the summers of 2000, 2003 and 2018 show that the main differences in the meteorological conditions were 1) higher temperatures in 2003 with respect to those in 2000 and 2018 which led to higher ozone concentrations in 2003; 2) higher fraction of air masses from high-ozone regions (from east in southern Switzerland and from north in northern Switzerland) are found in 2018, indicating the meteorological conditions in 2018 have an increasing effect on the ozone concentration. Therefore, the reduced anthropogenic emissions are the main reason responsible for the not-so-high ozone in the warm summer of 2018.

Data availability

Data in the figures are available online at https://doi.org/10.5281/zenodo.6474486.

CRediT authorship contribution statement

Hossein Zohdirad: Software, Formal analysis, Investigation, Writing – original draft, Writing – review & editing. **Jianhui Jiang:** Methodology, Software, Formal analysis, Writing – review & editing. **Sebnem Aksoyoglu:** Supervision, Writing – review & editing. **Masoud Montazeri Namin:** Writing – review & editing. **Khosro Ashrafi:** Writing – review & editing. **Andre S.H. Prevot:** Conceptualization, Supervision, Writing – review & editing.

Declaration of competing interest

The authors declare that they have no known competing financial interests or personal relationships that could have appeared to influence the work reported in this paper.

Acknowledgments

This study was financially supported by the Swiss Federal Office for the Environment (contract no. 16.0096.PJ/S291-1787) and Science and Technology Commission of Shanghai Municipality, China (Shanghai Pujiang Program, 21PJ1402800). Hossein Zohdirad would acknowledge the support of the mobility grant from the "Leading House South Asia and Iran, Zurich University of Applied Sciences". We would like to thank TNO for providing anthropogenic emissions, the European Centre for Medium-Range Weather Forecasts (ECMWF) for the access to the meteorological data, and the European Environmental Agency (EEA) and FOEN for the measured air quality and meteorological data. We acknowledge RAMBOLL for support in CAMx modeling. Simulation of WRF and CAMx were performed at the Swiss National Supercomputing Centre (CSCS) and the Merlin HPC Cluster at PSI.

Appendix A. Supplementary data

Supplementary data to this article can be found online at https://doi.org/10.1016/j.atmosenv.2022.119099.

References

Aksoyoglu, S., Keller, J., Ciarelli, G., Prévôt, A.S.H., Baltensperger, U., 2014. A model study on changes of European and Swiss particulate matter, ozone and nitrogen deposition between 1990 and 2020 due to the revised Gothenburg protocol. Atmos. Chem. Phys. 14, 13081–13095. https://doi.org/10.3929/ethz-b-000094759.

Andreani-Aksoyoglu, S., Keller, J., 1995. Estimates of monoterpene and isoprene emissions from the forests in Switzerland. J. Atmos. Chem. 20, 71–87. https://doi.org/10.1007/BF01099919.

Andreani-Aksoyoğlu, Ş., Keller, J., Ordóñez, C., Tinguely, M., Schultz, M., Prévôt, A.S.H., 2008. Influence of various emission scenarios on ozone in Europe. Ecol. Model. 217, 209–218. https://doi.org/10.1016/j.ecolmodel.2008.06.022.

Bessagnet, B., Pirovano, G., Mircea, M., Cuvelier, C., Aulinger, A., Calori, G., Ciarelli, G., Manders, A., Stern, R., Tsyro, S., 2016. Presentation of the EURODELTA III intercomparison exercise–evaluation of the chemistry transport models' performance on criteria pollutants and joint analysis with meteorology. Atmos. Chem. Phys. 16, 12667–12701. https://doi.org/10.5194/acp-16-12667-2016.

Bieser, J., Aulinger, A., Matthias, V., Quante, M., Denier van der Gon, H.A.C., 2011. Vertical emission profiles for Europe based on plume rise calculations. Environ. Pollut. 159, 2935–2946. https://doi.org/10.1016/j.envpol.2011.04.030.

Boleti, E., Hueglin, C., Takahama, S., 2018. Ozone time scale decomposition and trend assessment from surface observations in Switzerland. Atmos. Environ. 440–451. https://doi.org/10.1016/j.atmosenv.2018.07.039, 191.

Borrego, C., Monteiro, A., Martins, H., Ferreira, J., Fernandes, A.P., Rafael, S., Miranda, A.I., Guevara, M., Baldasano, J.M., 2016. Air quality plan for ozone: an urgent need for North Portugal. Air Qual., Atmos. Health 9, 447–460. https://doi.org/10.1007/s11869-015-0352-5.

Boylan, J.W., Russell, A.G., 2006. PM and light extinction model performance metrics, goals, and criteria for three-dimensional air quality models. Atmos. Environ. 40, 4946–4959. https://doi.org/10.1016/j.atmosenv.2005.09.087.

Brandt, J., Silver, J.D., Christensen, J.H., Andersen, M.S., Bønløkke, J.H., Sigsgaard, T., Geels, C., Gross, A., Hansen, A.B., Hansen, K.M., Hedegaard, G.B., Kaas, E., Frohn, L. M., 2013. Contribution from the ten major emission sectors in Europe and Denmark to the health-cost externalities of air pollution using the EVA model system – an integrated modelling approach. Atmos. Chem. Phys. 13, 7725–7746. https://doi.org/10.5194/acp-13-7725-2013.

CH2018, 2018. Climate Scenarios for Switzerland. National Centre for Climate Services, Zurich.

Coelho, S., Ferreira, J., Rodrigues, V., Rafael, S., Borrego, C., Lopes, M., 2017. Identification and analysis of source contributions to the air quality in the amsterdam region. WIT Trans. Ecol. Environ. 211, 31–40. https://doi.org/10.2495/AIR170031.

Cohan, D.S., Napelenok, S.L., 2011. Air quality response modeling for decision support. Atmosphere 2, 407–425. https://doi.org/10.3390/atmos2030407.

Colette, A., Granier, C., Hodnebrog, Ø., Jakobs, H., Maurizi, A., Nyiri, A., Bessagnet, B., D'Angiola, A., D'Isidoro, M., Gauss, M., Meleux, F., Memmesheimer, M., Mieville, A., Rouïl, L., Russo, F., Solberg, S., Stordal, F., Tampieri, F., 2011. Air quality trends in Europe over the past decade: a first multi-model assessment. Atmos. Chem. Phys. 11, 11657–11678. https://doi.org/10.5194/acp-11-11657-2011.

de Cámara, E.S., Gangoiti, G., Alonso, L., Valdenebro, V., Aksoyoglu, S., Oikonomakis, E., 2018. Ozone source apportionment to quantify local-to-continental source contributions to episodic events in northern Iberia. In: Air Pollution Modeling and its Application XXV, Cham, pp. 361–365. https://doi.org/10.1007/978-3-319-57645-9_57.

Derwent, R.G., Witham, C.S., Utembe, S.R., Jenkin, M.E., Passant, N.R., 2010. Ozone in Central England: the impact of 20 years of precursor emission controls in Europe. Environ. Sci. Pol. 13, 195–204. https://doi.org/10.1016/j.envsci.2010.02.001.

Derwent, R.G., Utembe, S.R., Jenkin, M.E., Shallcross, D.E., 2015. Tropospheric ozone production regions and the intercontinental origins of surface ozone over Europe. Atmos. Environ. 112, 216–224. https://doi.org/10.1016/j.atmosenv.2015.04.049.

Draxier, R.R., Hess, G.D., 1998. An overview of the HYSPLIT_4 modelling system for trajectories, dispersion and deposition. Aust. Meteorol. Mag. 47, 295–308.

Emery, C., Tai, E., Yarwood, G., 2001. Enhanced meteorological modeling and performance evaluation for two Texas ozone episodes. In: Final Report Submitted to Texas Natural Resources Conservation Commission, Prepared. ENVIRON. International Corp., Novato.

Guerreiro, C.B.B., Foltescu, V., de Leeuw, F., 2014. Air quality status and trends in Europe. Atmos. Environ. 98, 376–384. https://doi.org/10.1016/j.atmosenv.2014.09.017.

Guo, H., Jiang, F., Cheng, H.R., Simpson, I.J., Wang, X.M., Ding, A.J., Wang, T.J., Saunders, S.M., Wang, T., Lam, S.H.M., Blake, D.R., Zhang, Y.L., Xie, M., 2009. Concurrent observations of air pollutants at two sites in the Pearl River Delta and the implication of regional transport. Atmos. Chem. Phys. 9, 7343–7360. https://doi.org/10.5194/acp-9-7343-2009.

Henschel, S., Le Tertre, A., Atkinson, R.W., Querol, X., Pandolfi, M., Zeka, A., Haluza, D., Analitis, A., Katsouyanni, K., Bouland, C., Pascal, M., Medina, S., Goodman, P.G., 2015. Trends of nitrogen oxides in ambient air in nine European cities between 1999 and 2010. Atmos. Environ. 117, 234–241. https://doi.org/10.1016/j.atmosenv.2015.07.013.

Hess, P.G., Zbinden, R., 2013. Stratospheric impact on tropospheric ozone variability and trends: 1990–2009. Atmos. Chem. Phys. 13, 649–674. https://doi.org/10.5194/acp-13-649-2013.

Hong, S.-Y., Noh, Y., Dudhia, J., 2006. A new vertical diffusion package with an explicit treatment of entrainment processes. Mon. Weather Rev. 134, 2318–2341. https://doi.org/10.1175/MWR3199.1.

Jacob, D.J., Winner, D.A., 2009. Effect of climate change on air quality. Atmos. Environ. 43, 51–63. https://doi.org/10.1016/j.atmosenv.2008.09.051.

Jenkin, M.E., 2008. Trends in ozone concentration distributions in the UK since 1990: local, regional and global influences. Atmos. Environ. 42, 5434–5445. https://doi.org/10.1016/j.atmosenv.2008.02.036.

Jiang, J., Aksoyoglu, S., Ciarelli, G., Oikonomakis, E., El-Haddad, I., Canonaco, F., O'Dowd, C., Ovadnevaite, J., Minguillón, M.C., Baltensperger, U., Prévôt, A.S.H., 2019. Effects of two different biogenic emission models on modelled ozone and aerosol concentrations in Europe. Atmos. Chem. Phys. 19, 3747–3768. https://doi.org/10.5194/acp-19-3747-2019.

Jiang, J., Aksoyoglu, S., Ciarelli, G., Baltensperger, U., Prévôt, A.S.H., 2020. Changes in ozone and PM2. 5 in Europe during the period of 1990–2030: role of reductions in land and ship emissions. Sci. Total Environ. 741, 140467 https://doi.org/10.1016/j.scitotenv.2020.140467.

Jonson, J.E., Simpson, D., Fagerli, H., Solberg, S., 2006. Can we explain the trends in European ozone levels? Atmos. Chem. Phys. 6, 51–66. https://doi.org/10.5194/acp-6-51-2006.

Jonson, J.E., Schulz, M., Emmons, L., Flemming, J., Henze, D., Sudo, K., Lund, M.T., Lin, M., Benedictow, A., Koffi, B., 2018. The effects of intercontinental emission sources on European air pollution levels. Atmos. Chem. Phys. 18, 13655–13672. https://doi.org/10.5194/acp-18-13655-2018.

Karamchandani, P., Long, Y., Pirovano, G., Balzarini, A., Yarwood, G., 2017. Source-sector contributions to European ozone and fine PM in 2010 using AQMEII modeling data. Atmos. Chem. Phys. 17, 5643–5664. https://doi.org/10.5194/acp-17-5643-2017.

Kuenen, J.J.P., Visschedijk, A.J.H., Jozwicka, M., Denier Van Der Gon, H.A.C., 2014. TNO-MACC_II emission inventory; a multi-year (2003–2009) consistent high-resolution European emission inventory for air quality modelling. Atmos. Chem. Phys. 14, 10963–10976. https://doi.org/10.5194/acp-14-10963-2014.

Kwok, R.H.F., Baker, K.R., Napelenok, S.L., Tonnesen, G.S., 2015. Photochemical grid model implementation and application of VOC, NO_x, and O_3 source apportionment. Geosci. Model Dev. 8, 99–114. https://doi.org/10.5194/gmd-8-99-2015.

Lamarque, J.-F., Emmons, L.K., Hess, P.G., Kinnison, D.E., Tilmes, S., Vitt, F., Heald, C.L., Holland, E.A., Lauritzen, P.H., Neu, J., 2012. CAM-chem: description and evaluation of interactive atmospheric chemistry in the community earth system model. Geosci. Model Dev. 5, 369–411. https://doi.org/10.5194/gmd-5-369-2012.

Li, Y., Lau, A.K.-H., Fung, J.C.-H., Zheng, J.Y., Zhong, L.J., Louie, P.K.K., 2012. Ozone source apportionment (OSAT) to differentiate local regional and super-regional source contributions in the Pearl River Delta region, China. J. Geophys. Res. Atmos. 117 https://doi.org/10.1029/2011JD017340.

Li, N., He, Q., Greenberg, J., Guenther, A., Li, J., Cao, J., Wang, J., Liao, H., Wang, Q., Zhang, Q., 2018. Impacts of biogenic and anthropogenic emissions on summertime ozone formation in the Guanzhong Basin, China. Atmos. Chem. Phys. 18, 7489–7507. https://doi.org/10.5194/acp-18-7489-2018.

Lupaşcu, A., Butler, T., 2019. Source attribution of European surface O_3 using a tagged O_3 mechanism. Atmos. Chem. Phys. 19, 14535–14558. https://doi.org/10.5194/acp-19-14535-2019.

Mertens, M., Grewe, V., Rieger, V.S., Jöckel, P., 2018. Revisiting the contribution of land transport and shipping emissions to tropospheric ozone. Atmos. Chem. Phys. 18, 5567–5588. https://doi.org/10.5194/acp-18-5567-2018.

Mertens, M., Kerkweg, A., Grewe, V., Jöckel, P., Sausen, R., 2020. Attributing ozone and its precursors to land transport emissions in Europe and Germany. Atmos. Chem. Phys. 20, 7843–7873. https://doi.org/10.5194/acp-20-7843-2020.

Monks, P.S., 2005. Gas-phase radical chemistry in the troposphere. Chem. Soc. Rev. 34, 376–395. https://doi.org/10.1039/B307982C.

Monks, P.S., Archibald, A.T., Colette, A., Cooper, O., Coyle, M., Derwent, R., Fowler, D., Granier, C., Law, K.S., Mills, G.E., Stevenson, D.S., Tarasova, O., Thouret, V., von Schneidemesser, E., Sommariva, R., Wild, O., Williams, M.L., 2015. Tropospheric ozone and its precursors from the urban to the global scale from air quality to short-lived climate forcer. Atmos. Chem. Phys. 15, 8889–8973. https://doi.org/10.5194/acp-15-8889-2015.

NCAR, 2016. Weather Research and Forecasting Model WRF-ARW Version 3 Modeling System User's Guide. National Center for Atmospheric Research, Boulder, Colorado, USA.

Oderbolz, D.C., Aksoyoglu, S., Keller, J., Barmpadimos, I., Steinbrecher, R., Skjøth, C.A., Plaß-Dülmer, C., Prévôt, A.S.H., 2013. A comprehensive emission inventory of biogenic volatile organic compounds in Europe: improved seasonality and land-cover. Atmos. Chem. Phys. 13, 1689–1712. https://doi.org/10.5194/acp-13-1689-2013.

Oikonomakis, E., Aksoyoglu, S., Ciarelli, G., Baltensperger, U., Prévôt, A.S.H., 2018. Low modeled ozone production suggests underestimation of precursor emissions (especially NO_x) in Europe. Atmos. Chem. Phys. 18, 2175–2198. https://doi.org/10.5194/acp-18-2175-2018.

Ordóñez, C., Mathis, H., Furger, M., Henne, S., Hüglin, C., Staehelin, J., Prévôt, A.S.H., 2005. Changes of daily surface ozone maxima in Switzerland in all seasons from 1992 to 2002 and discussion of summer 2003. Atmos. Chem. Phys. 5, 1187–1203. https://doi.org/10.5194/acp-5-1187-2005.

Passant, N.R., 2002. Speciation of UK Emissions of Non-methane Volatile Organic Compounds. AEA Technology.

Pay, M.T., Pando, C.P.-G., Guevara, M., Jorba, O., Napelenok, S., Querol, X., 2018. Unravelling the origin of high ozone concentrations in southwestern Europe. In: International Technical Meeting on Air Pollution Modelling and its Application, pp. 17–21.

Pay, M.T., Gangoiti, G., Guevara, M., Napelenok, S., Querol, X., Jorba, O., Pérez García-Pando, C., 2019. Ozone source apportionment during peak summer events over southwestern Europe. Atmos. Chem. Phys. 19, 5467–5494. https://doi.org/10.5194/acp-19-5467-2019.

Ramboll, 2018. User's Guide: the Comprehensive Air Quality Model with Extensions (CAMx) Version 6.5, California.

Safieddine, S., Boynard, A., Coheur, P.-F., Hurtmans, D., Pfister, G., Quennehen, B., Thomas, J.L., Raut, J.-C., Law, K.S., Klimont, Z., Hadji-Lazaro, J., George, M., Clerbaux, C., 2014. Summertime tropospheric ozone assessment over the Mediterranean region using the thermal infrared IASI/MetOp sounder and the WRF-Chem model. Atmos. Chem. Phys. 14, 10119–10131. https://doi.org/10.5194/acp-14-10119-2014.

Schär, C., Vidale, P.L., Lüthi, D., Frei, C., Häberli, C., Liniger, M.A., Appenzeller, C., 2004. The role of increasing temperature variability in European summer heatwaves. Nature 427, 332–336. https://doi.org/10.1038/nature02300.

Sudo, K., Akimoto, H., 2007. Global source attribution of tropospheric ozone: long-range transport from various source regions. J. Geophys. Res. Atmos. 112 https://doi.org/10.1029/2006JD007992.

Tang, W., Cohan, D.S., Morris, G.A., Byun, D.W., Luke, W.T., 2011. Influence of vertical mixing uncertainties on ozone simulation in CMAQ. Atmos. Environ. 45, 2898–2909. https://doi.org/10.1016/j.atmosenv.2011.01.057.

Teixeira, E., Fischer, G., van Velthuizen, H., van Dingenen, R., Dentener, F., Mills, G., Walter, C., Ewert, F., 2011. Limited potential of crop management for mitigating

surface ozone impacts on global food supply. Atmos. Environ. 45, 2569–2576. https://doi.org/10.1016/j.atmosenv.2011.02.002.

Valverde, V., Pay, M.T., Baldasano, J.M., 2016. Ozone attributed to Madrid and barcelona on-road transport emissions: characterization of plume dynamics over the Iberian Peninsula. Sci. Total Environ. 543, 670–682. https://doi.org/10.1016/j.scitotenv.2015.11.070.

Wang, X., Li, J., Zhang, Y., Xie, S., Tang, X., 2009. Ozone source attribution during a severe photochemical smog episode in Beijing, China. Sci. China, Ser. B: Chemistry 52, 1270–1280.

WHO, 2013. Review of Evidence on Health Aspects of Air Pollution – REVIHAAP Project: Final Technical Report.